20th Australasian Fluid Mechanics Conference
Perth, Australia
5-8 December 2016

Coherent structures in a self-similar adverse pressure gradient turbulent boundary layer

A. Sekimoto[1], V. Kitsios[1], C. Atkinson[1], J. Jiménez[2] and J. Soria[1,3]

[1]Laboratory for Turbulence Research in Aerospace and Combustion, Department of Mechanical and Aerospace Engineering
Monash University, Clayton Campus, Melbourne, VIC 3800, Australia

[2]School of Aeronautics
Universidad Politécnica de Madrid, Pz Cardenal Cisneros 3, 28040 Madrid, Spain

[3]Department of Aeronautical Engineering
King Abdulaziz University, Jeddah 21589, Kingdom of Saudi Arabia

Abstract

The turbulence statistics and structures of a self-similar adverse pressure gradient turbulent boundary layer (APG-TBL) at the verge of separation are investigated using a direct numerical simulation (DNS). The desired self-similar APG-TBL is achieved by a modification of the far-field velocity boundary condition. The required wall-normal velocity in the far-field to produce the necessary adverse pressure gradient was estimated based on the analytical free-stream streamwise velocity distribution for a flow at the point of separation, and the assumption that the streamlines of the outer flow follow the growth of the boundary layer thickness. The APG-TBL develops over a momentum thickness based Reynolds number upto 12000, and achieves a self-similar region of constant friction coefficient, pressure velocity and shape factor. Turbulence statistics in this region show self-similar collapse when scaled by the external velocity and the displacement thickness. In this study, the coherent structures of a self-similar APG-TBL are investigated by using topological methodology and visualisation techniques.

Introduction

The turbulent boundary layer (TBL) subjected to strong adverse pressure gradient (APG) is frequently found to be challenging to predict particularly flow separation, with turbulence models performing poorly. In APG-TBL, many aspects of turbulent structures and the scaling of turbulence statistics remain unresolved. The canonical APG-TBL at the verge of separation is self-similar, in the sense that each of the term in the governing equations has the same proportionality with streamwise position [16, 15, 9]. After introducing numerical methods briefly, the coherent structures are investigated by using topological methodology [2, 13, 14] and three-dimensional flow visualisation.

Numerical methodology

The boundary layer is simulated in a three-dimensional rectangular domain over a no-slip smooth wall. The axes in the streamwise, wall-normal and spanwise directions are x, y and z. The corresponding velocity fluctuation with respect to the time-averaged mean (U, V, W) are (u, v, w). The spanwise boundary condition is periodic, and the Fourier expansion with $2/3$ dealiasing is applied. Compact finite differences in staggered grids are used in x and y [7]. The direct numerical simulation (DNS) is performed with a modification of the code of Borrel *et al.* [1, 12]. We use a modified version of the recycling method used by Sillero *et al.* [11], and the desired self-similar APG-TBL is achieved by a modification of the far-field velocity boundary condition. The required wall-normal velocity in the far-field to produce the necessary adverse pressure gradient was estimated based on the analytical free-stream streamwise velocity distribution for a flow at the point of separation [9]

$$U_e(x) \propto x^m \quad \text{with } m = -0.23, \tag{1}$$

and the assumption that the streamlines of the outer flow follow the growth of the boundary layer thickness. Further details of this methodology can be found in Kitsios et al. [6].

The reference velocity,

$$U_e(x) \equiv U_\Omega(x,\infty), \quad \text{where } U_\Omega(x,y) \equiv -\int_0^\infty \Omega_z(x,y')\mathrm{d}y' \tag{2}$$

and Ω_z is the mean spanwise vorticity. The displacement thickness and momentum thickness are defined by

$$\delta_1(x) = \frac{-1}{U_e}\int_0^\infty y\Omega_z(x,y)\mathrm{d}y \tag{3}$$

$$\delta_2(x) = \frac{2}{U_e^2}\int_0^\infty yU_\Omega\Omega_z(x,y)\mathrm{d}y - \delta_1(x) \tag{4}$$

The numerical details are summarised in table 1. The reference displacement thickness is $\delta_1(x^\star)$ at the streamwise position $x^\star$, at which the Reynolds number is $Re_{\delta_1}(x^\star) \equiv U_e\delta_1/\nu = 4800$, where ν is the kinematic viscosity. The boundary layer thickness in APG-TBL grows drastically, and it requires a larger L_y and more grid points in y direction (N_y) than those required for a zero-pressure-gradient turbulent boundary layer (ZPG-TBL).

By using the above reference velocity and outer scale, U_e and δ_1, the turbulence statistics of the strong APG-TBL collapses within the domain of interest as shown by red lines in figure 1. The data of ZPG-TBL at $x^\star$ and a channel database at $Re_\tau \approx 4200$ [8], whose displacement thickness is $\delta_1 = 0.094h$ from eq. (3), are also shown as a reference by the black and blue lines, respectively. It is indicated that velocity fluctuations in strong APG-TBL, which does not have logarithmic mean-velocity region, are mainly produced in the outer layer.

Characterisation of adverse pressure gradient turbulent boundary layer

The driving mechanism of the self-sustaining turbulence in strong APG-TBL is the local shear, as in the wall-bounded turbulence [5], so that the characteristics of the local mean shear rate both in APG-TBL and other wall-bounded flows are of great interest. Figure 2 shows the Corrsin shear parameter [4], $S^* \equiv (\partial U/\partial y)q^2/\varepsilon$, where $q^2 \equiv u^2+v^2+w^2$, as a function of $y/\delta_1(x)$ and ε is the turbulent dissipation rate. The nondimensional parameter is $S^* \approx 7$–9 both in homogeneous shear turbulence [10] and in the logarithmic layer of wall-bounded

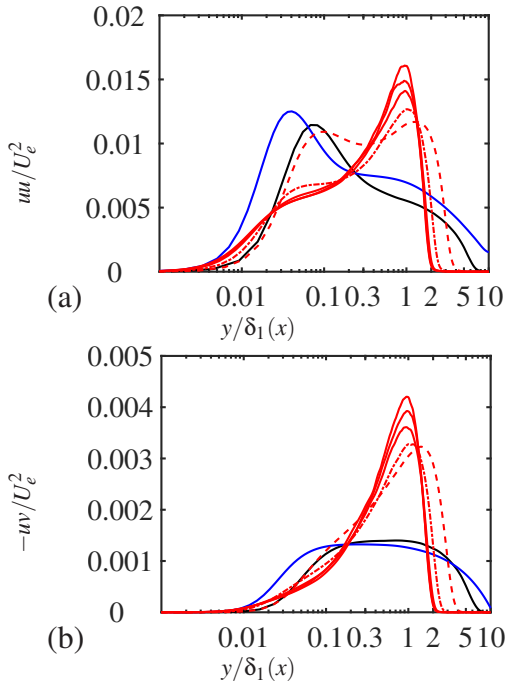

Figure 1: (a) The streamwise velocity fluctuation uu, (b) the Reynolds stress $-uv/U_e^2$ as a function of $y/\delta_1(x)$: (black) ZPG-TBL at x_{DoI}; (blue) channel turbulence at $Re_\tau \approx 4200$ [8]; (red) strong APG-TBL at $x = x^\star$ (dashed), $(x^\star + x_{\mathrm{DoI}})/2$ (dash-dotted). The solid lines are at x_{DoI}, at the middle- and end-point of the domain of interest.

flows [5, 8]. The near-wall peak of APG-TBL decreases as the layer grows, and the weaker local mean shear close to the wall would generate fewer turbulence structures. On the other hand, in the outer region $y/\delta_1 \approx 1$, S^* is roughly constant value at $y/\delta_1 \approx 1$, as in the logarithmic layer of ZPG-TBL or channel turbulence.

The topological methodology is applied at each y/δ_1 of APG-TBL and they are compared with those in ZPG-TBL. Figure 3 and 4 show the joint probability density function of the second and third invariant of the velocity gradient tensor, which clearly indicates that the dissipative fine-scale vortices are generated at $y/\delta_1 \approx 1$ in APG-TBL.

The instantaneous three-dimensional geometry of the self-similar APG is visualised in figure 5 and 6. The isosurfaces of intense Reynolds stress seem to be separated from the wall and that is also the case for the fine-scale vortex clusters represented by isosurfaces of the second invariant of the velocity gradient tensor. The two-point streamwise velocity correlation at $y/\delta_1 = 1$ (not shown) is shorter than that in ZPG-TBL and more inclined with respect to the wall in APG-TBL.

Conclusions and discussions

The direct numerical simulation of a self-similar APG-TBL at the verge of separation is performed and the coherent structures are investigated, using topological methodology and flow visualisation. The large-scale uv-structures, which are separated from the wall (so-called detached eddies), are observed in the self-similar APG-TBL, and it is revealed that most of the energy production is at around $y/\delta_1 \approx 1$. The streamwise correlation is much shorter in the streamwise direction than that of ZPG-TBL (not shown), and more inclined with respect to the wall in APG-TBL. The spanwise wavelength of the large-scale motion is also

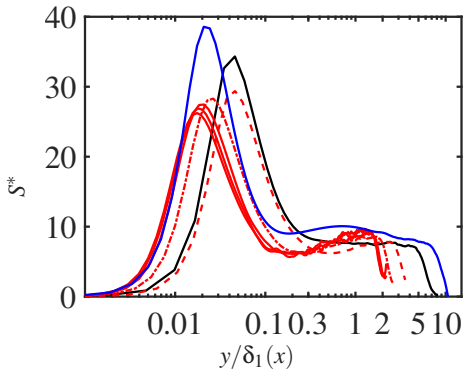

Figure 2: The same as figure 1, but for the Corrsin shear parameter [4], $S^* \equiv (\partial U/\partial y)q^2/\varepsilon$, where $q^2 \equiv u^2 + v^2 + w^2$, as a function of $y/\delta_1(x)$. The shear parameter is $S^* \approx 7$–9 both in homogeneous shear turbulence [10] and in the logarithmic layer of wall-bounded flows [8].

scaled by an outer scale unit (not shown), displacement thickness in this study, $\lambda_z \approx \delta_1$. The outer region at $y \approx \delta_1$ is very active in APG-TBL. In contrast, such an active dissipative region is close to the wall, from the buffer layer to logarithmic layer in ZPG-TBL. The local mean shear contributes to the energy production and organisation of large-scale motions. The kinetic energy production and the energy dissipation are balanced almost at the same height from the wall, which is illustrated in the three-dimensional visualisation of figure 6. In strong APG-TBL, dissipative small-scale structures are associated with the large-scale structure mainly at around $y/\delta_1 \approx 1$. Since most of events happens away from wall, the wall restriction on the flow structures in APG-TBL are much weaker than that in ZPG-TBL or channels. Further investigations on the coherent structures in the self-similar APG-TBL, in comparison with the other shear flows, are on-going.

Acknowledgements

The support of the ARC, NCI and Pawsey SCC funded by the Australian and Western Australian governments as well as the support of PRACE funded by the European Union are gratefully acknowledged.

References

[1] Borrel, G., Sillero, J. A. and Jiménez, J., A code for direct numerical simulation of turbulent boundary layers at high Reynolds numbers in BG/P supercomputers, *Comp. Fluids*, **80**, 2013, 37–43.

[2] Chong, M., Soria, J., Perry, A., Chacin, J., Cantwell, B. and Na, Y., Turbulence structures of wall-bounded shear flows found using DNS data, *J. Fluid Mech.*, **357**, 1998, 225–247.

[3] Clauser, F. H., Turbulent boundary layers in adverse pressure gradients, *J. Aero. Sci.*, **21**, 1954, 91–108.

[4] Corrsin, S., Local isotropy in turbulent shear flow, *NACA Research Memo.*, **58B11**.

[5] Jiménez, J., Near-wall turbulence., *Phys. Fluids*, **25**, 2013, 101302.

[6] Kitsios, V., Sekimoto, A., Atkinson, C., Sillero, J., Borrell, G., Gungor, A. G., Jiménez, J. and Soria, J., Direct numerical simulation of a self-similar adverse pressure

Table 1: Numerical details of the ZPG-TBL and self-similar APG-TBL. β represents non-dimensional pressure gradient as proposed by Clauser [3]. Number of collocation points in the streamwise (N_x) and wall normal (N_y) direction, and the number of Fourier modes in the spanwise (N_z) direction; the computational domain (L_x, L_y, L_z) relative to the displacement thickness (δ_1) at the position $x^\star$, where $Re_{\delta 1} = 4800$; the upstream position of the domain of interest (DoI), x_{DoI}; the streamwise length of DoI, L_{DoI}. The variation of δ_1, shape factor H and $Re_{\delta 1}$ in DoI are also shown.

	ZPG($\beta = 0$)			APG ($\beta = 39$)		
(N_x, N_y, N_z)	8193	315	1362	8193	1000	1362
$(L_x, L_y, L_z)/\delta_1(x^\star)$	480	22.7	80.1	297	72.0	49.6
$x_{\mathrm{DoI}}/\delta_1(x^\star), L_{\mathrm{DoI}}/\delta_1(x^\star), L_{\mathrm{DoI}}/\delta_1(x_{\mathrm{DoI}})$	0	80.9	80.9	94.9	36.3	6.43
$\delta_1/\delta_1(x^\star)$ range in DoI	$1.0 \rightarrow 1.11$			$5.63 \rightarrow 7.57$		
$H(x^\star)$, H range in DoI	1.37			1.68	$2.22 \rightarrow 2.35$	
$Re_{\delta 1}(x^\star)$, $Re_{\delta 1}$ range in DoI	4800	$4800 \rightarrow 5280$		4800	$22200 \rightarrow 28800$	

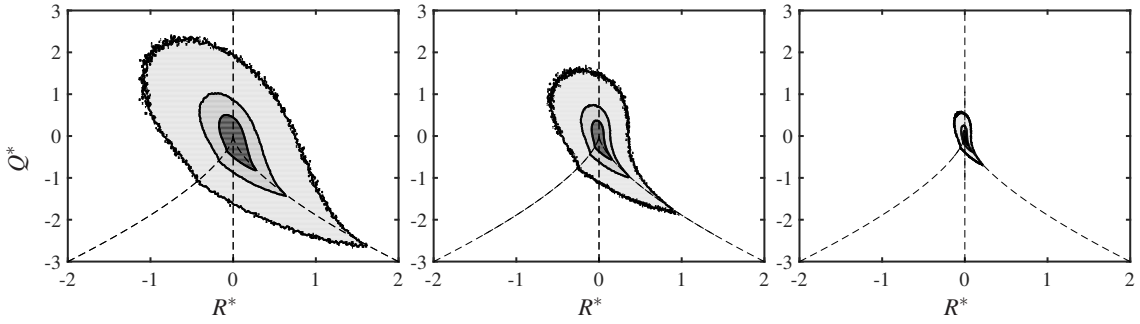

Figure 3: Joint probability density function between $Q^* = Q/(U_e/\delta_1)^2$ and $R^* = R/(U_e/\delta_1)^3$ for ZPG-TBL with $Re_{\delta 1} \approx 5000$ in (left) buffer layer, $y/\delta_1 \approx 0.1$ (centre) logarithmic layer, $y/\delta_1 \approx 0.3$ (right) outer region $y/\delta_1 \approx 1.0$. The iso-probability contours are 60%, 80%, and 95% of the data. The data is averaged in the domain of interest.

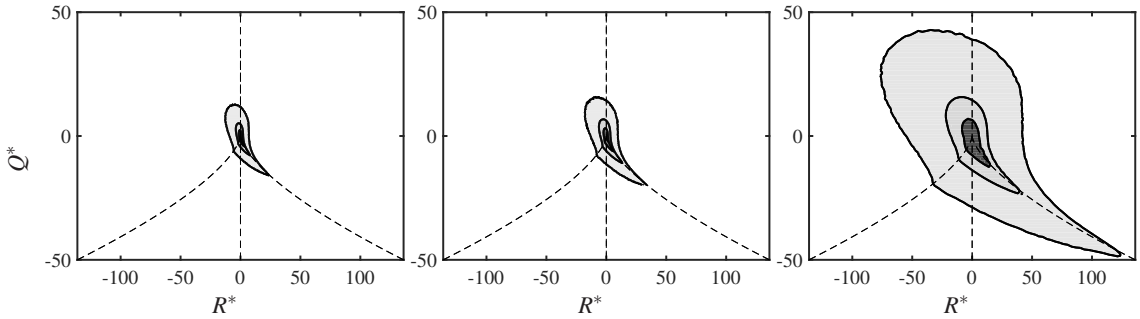

Figure 4: The same with figure 3, but for self-similar APG-TBL with $Re_{\delta 1} \approx 25000$ in (left) $y/\delta_1 \approx 0.1$ (center) $y/\delta_1 \approx 0.3$ (right) outer region, $y/\delta_1 \approx 1.0$. The data is the streamwise average in the domain of interest, assuming the self-similarity.

gradient turbulent boundary layer at the verge of separation, *(in preparation)*.

[7] Lele, S. K., Compact finite difference schemes with spectral-like resolution, *J. Comput. Phys.*, **103**, 1992, 16–42.

[8] Lozano-Durán, A. and Jiménez, J., Effect of the computational domain on direct simulations of turbulent channels up to $Re_\tau = 4200$., *Phys. Fluids*, **26**, 2014, 011702.

[9] Mellor, G. L. and Gibson, D. M., Equilibrium turbulent boundary layers, *J. Fluid Mech.*, **24**, 1966, 225–253.

[10] Sekimoto, A., Dong, S. and Jiménez, J., Direct numerical simulation of statistically stationary and homogeneous shear turbulence and its relation to other shear flows, *Phys. Fluids*, **28**, 2016, 035101.

[11] Sillero, J. A., Jiménez, J. and Moser, R. D., One-point statistics for turbulent wall-bounded flows at Reynolds numbers up to $\delta^+ \approx 2000$, *Phys. Fluids*, **25**, 2013, 105102.

[12] Simens, M., Jiménez, J., Hoyas, S. and Mizuno, Y., A high-resolution code for turbulent boundary layers, *J. Comp. Phys.*, **228**, 2009, 4128–4231.

[13] Soria, J. and Cantwell, B. J., Topological visualisation of focal structures in free shear flows, *Appl. Sci. Res.*, **53**, 1994, 375–386.

[14] Soria, J., Sondergaard, R., Cantwell, B., Chong, M. and Perry, A., A study of the fine-scale motions of incompressible time-developing mixing layers, *Phys. Fluids*, **6**, 1994, 871–884.

[15] Townsend, A., The development of turbulent boundary layers with negligible wall stress, *J. Fluid Mech.*, **8**, 1960, 143–155.

[16] Townsend, A. A., *The Structure of Turbulent Shear Flows, 2nd ed.*, Cambridge U. Press, 1976.

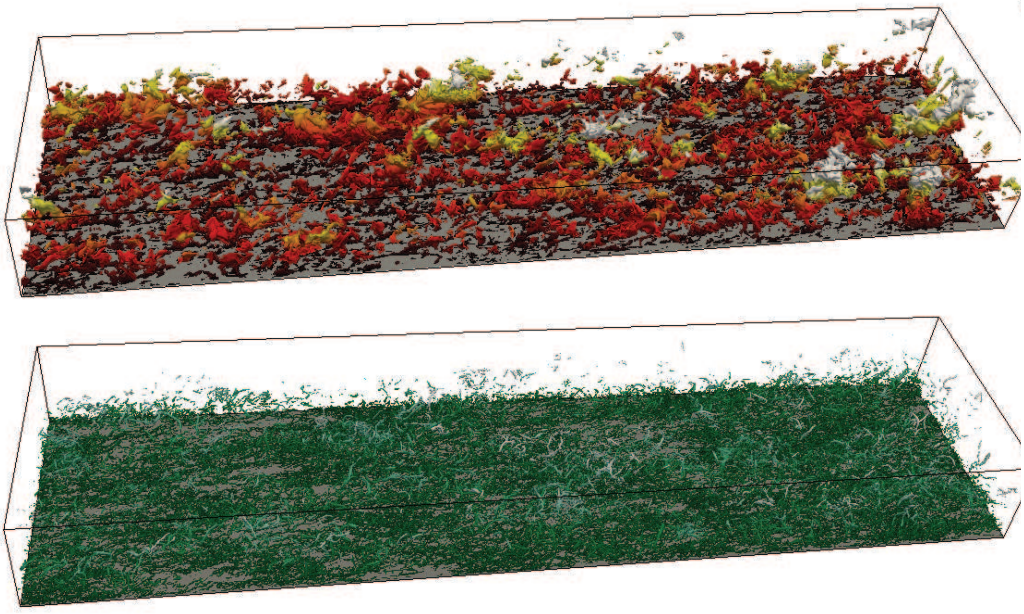

Figure 5: The region of intense Reynolds stress (left, red) and the second invariant of the velocity gradient tensor (right, green) in ZPG-TBL. Only the full domain of interest $[L_{DoI}, 0.38L_y, L_z/4] = [80.9, 8.6, 19.9]\delta_1(x^\star)$ is shown. The threshold for the isosurfaces is $-uv/U_e^2 = 0.006$, which is 4 times larger than the peak value in the buffer layer of ZPG-TBL, and $Q^* = Q/(U_e/\delta_1)^2 = 0.5$ (see figure 3). δ_1 grows 11% within the domain of interest as in table 1. The flow is from left to right. The colourmap of isosurfaces is the distance from the wall, and the white colour represents $6\delta_1(x)$.

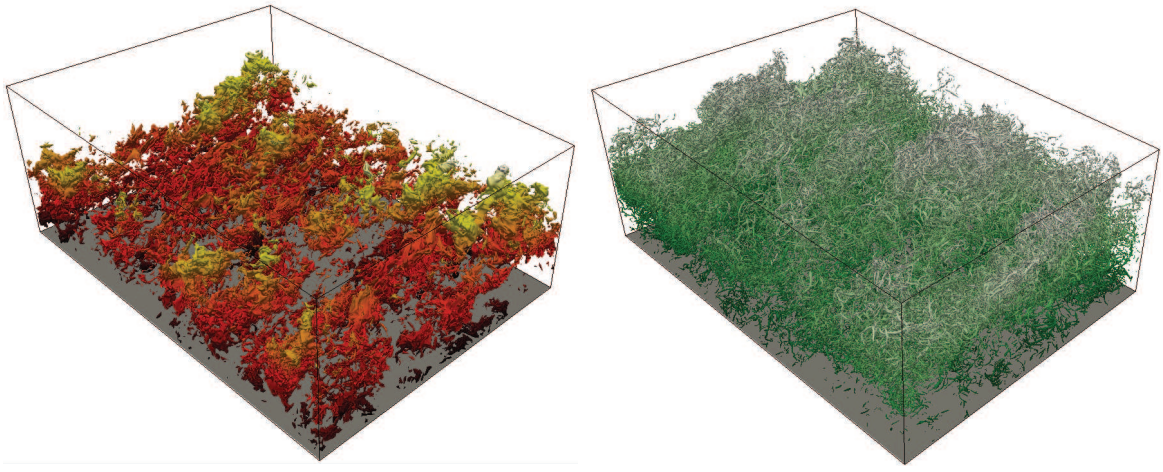

Figure 6: The region of intense Reynolds stress (left, red) and the second invariant of the velocity gradient tensor (right, green) in the self-similar APG-TBL. Only a quarter of the domain of interest $[L_{DoI}, 0.27L_y, L_z] = [36.3, 19.3, 50.7]\delta_1(x^\star) = [6.4, 3.43, 8.8]\delta_1(x_{\mathrm{DoI}})$ is shown. The threshold for the isosurfaces is $-uv/U_e^2 = 0.016$, which is 4 times larger than the outer peak of APG-TBL, and $Q^* = Q/(U_e/\delta_1)^2 = 25$ (see figure 4). Note that the free-stream velocity U_e and outer length scale δ_1 is a function of the streamwise position x, and δ_1 grows 34% within the DoI. The flow is from left to top-right. The colourmap of isosurfaces is the distance from the wall, and the white colour represents $3\delta_1(x)$.